



*Keywords:* Freak; Wave; Nonlinear; Set-down; NewWave.

## **1. Introduction**

The Draupner platform is situated in the Norwegian sector of the North Sea in water of 70m depth. Two twenty minute surface elevation time series from the Draupner platform were considered in this study, each having an average wave period,  $T_z$ , of 12.5 seconds, corresponding to an average frequency,  $f_z$ , of 0.08Hz. The first time series, recorded from 15:20 on the 1<sup>st</sup> January 1995, contains the New Year wave, and the second was recorded one hour later from 16:20. Henceforth these two wave records will be referred to as Draupner 1520 and 1620 data sets. The data were measured using a downward looking laser device. The significant wave heights for the 1520 and 1620 data sets are 11.92m and 12.04m respectively and the sampling rate for both is 2.1Hz. Previous analyses of freak waves with reference to the New Year wave has been undertaken by Haver and Jan Andersen [3] and Prevosto and Bouffandeau [4].

The time series plots for the two Draupner wave records are shown in Figure 1. The data analysed display obvious nonlinear behaviour. The shapes of the crests are consistently sharper and larger than their trough equivalents. A ‘design wave’ called NewWave is shown to be an acceptable local model for the linear contribution to large waves in these data sets. Waves in nature are, however, nonlinear, and so higher order effects are assessed both through the introduction of simple Stokes-type corrections and the implementation of exact second order wave theory (Dean and

Sharma [5], Dalzell [6]). Furthermore, spectral analysis is used to identify unique features of the New Year wave distinguishing it from a typical large wave.

## **2. Crest-trough comparison**

Average large crest and trough profiles for the two studied data sets, computed using the largest 50% of crest and troughs, are shown in Figure 2. These profiles are obtained by extracting the local time history around each large crest and trough, resetting the time series so that peak crest elevation and peak trough depression occur at zero time, and then averaging across all the time series. As one would expect, the results presented show that the crests are higher and spikier, and the troughs are less deep and more rounded. The New Year wave is omitted from this averaging process because it is so extreme compared to all other waves in either record.

Qualitatively, the apparent asymmetry between crests and troughs for free surface waves is the most obvious manifestation of nonlinearity in the ocean, and this effect has been observed unambiguously in the data studied here. The magnitude of this effect can be illustrated by sorting the peak crest elevations and peak trough depressions into ascending order and then plotting the  $n^{\text{th}}$  largest crest against the  $n^{\text{th}}$  largest trough. Such plots for the two Draupner wave records are shown in Figure 3, where a dashed 1:1 line has been included to help illustrate the asymmetry of the waves. It is worth emphasising that there is no particular temporal relationship between the  $n^{\text{th}}$  largest crest and the  $n^{\text{th}}$  largest trough.

Both data sets produce largely predictable results, with crest-trough asymmetry increasing as the size of the crests and troughs increase. It is perhaps curious to note that for very small crests and troughs (with an elevation or depression  $< \sim 1\text{m}$ ) the size of the trough depression is actually greater than the corresponding crest elevation on average. Uncertainty in the true location of the mean sea level could perhaps be the cause of this. Indeed, when handling time series containing a relatively small number of waves, averaging should take place over an integer number of periods when removing any tidal contribution, otherwise small errors can be introduced.

A major drawback to presenting such results for the Draupner data is that there are comparatively few instances of large waves within the data. Hence, towards the top end of such ordered data sets, there is considerable sample variability.

### **3. NewWave Comparison**

In regions such as the North Sea and the Gulf of Mexico the design of offshore structures is principally concerned with the environmental loads and peak surface elevations generated by extreme storms. As an alternative to running many hours of random time domain simulation, a convenient ‘design-wave’ based on the average shape of an extreme in a linear random Gaussian process can be used (Lindgren [1] and Boccotti [2]). In offshore engineering this ‘design-wave’ has become known as NewWave. The linear NewWave is simply proportional to the auto-correlation function, which is the Fourier transform of the power spectrum:

$$\rho(\tau) = \frac{1}{\sigma^2} \int_0^{\infty} S_{\eta\eta}(\omega) \cdot \cos(\omega\tau) d\omega \quad (1)$$

where  $\sigma$  is the standard deviation of the wave record and  $S_{\eta\eta}(\omega)$  is the power spectral density. The shape of the NewWave, as described by equation (1), can be discretised by a sum of a finite number,  $N$ , of sinusoidal components. For completeness, the definition is now extended to include spatial dependence, but limiting this to uni-directional seas. The discretised NewWave can be written as:

$$\eta(X, \tau) = \frac{\alpha}{\sigma^2} \sum_{n=1}^N S_{\eta\eta}(\omega_n) \cdot d\omega \cdot \cos(k_n X - \omega_n \tau), \quad (2)$$

where  $X = x - x_0$  is the distance relative to the point of occurrence of the large crest;  $\tau = t - t_0$ , the time relative to the time of occurrence of the large crest;  $\alpha$  is the linear crest amplitude (which can be estimated using the Rayleigh distribution) and  $k_n$  is the wavenumber of the  $n^{\text{th}}$  sinusoidal component. NewWave hence models the broad-banded character of large ocean waves as a set of independent freely propagating sinusoidal components of different amplitude. A linear NewWave involves the superposition of these components with an extreme crest being generated when all the components come into phase. The NewWave profile will now be compared against the average linear large crest profile for the two Draupner data sets.

From a consideration of a Stokes water wave expansion, it can be easily shown that the odd harmonics (which will be dominated by the linear contribution) can be readily extracted from a time series using the expression:

$$\eta_{odd} = \frac{\eta_C - \eta_T}{2} \quad (3)$$

where  $\eta_C$  is the average large crest profile (crest elevation taken as positive) and  $\eta_T$  is the average large trough profile (trough depression taken as negative). To obtain  $\eta_C$  and  $\eta_T$  the largest 50% of crests and troughs have been averaged, again with the New Year wave omitted.

Figure 4 compares the scaled  $\eta_{odd}$  profile (which is approximately the average linear profile) with the NewWave profile computed using equation (2) for the two Draupner wave records. The New Year has been excluded for this comparison since one cannot expect its second order components to be removed using equation (3). The agreement is reasonable in the local vicinity of the extreme peaks although large variability develops away from  $t=0$ . One discrepancy is that the central peaks of  $\eta_{odd}$  profiles are slightly narrower for both the 1520 and 1620 data sets. This is likely to be caused by the third order harmonic contribution retained in  $\eta_{odd}$ . The large differences between the data averages and NewWave found well away from  $t=0$  for both data sets can be attributed to statistical variability, as there are a comparatively small number of large waves in each record. NewWave has been extensively verified for field data in both deep and shallow water (Jonathan and Taylor [7], Taylor and Williams [8]), so it is reasonable to conclude that NewWave is a valid model for the underlying linear data and that the discrepancies observed are the result of statistical variability and/or a large third harmonic contribution. Later the NewWave profile is modified to incorporate nonlinear corrections up to fifth order and a comparison is made with the New Year wave profile.

#### 4. Second and third order corrections

Attention is now turned to the nonlinear contributions to a wave record not considered thus far. Stokes-type corrections are presented as a means of approximating the second and third order contributions to a wave record. An alternative approach would be to use the exact second order interaction kernel of Dean and Sharma [5], and Dalzell [6], and this will also be discussed later. Here a technique is outlined that enables the second and third order sum contributions to a wave record to be temporally decomposed.

The first three terms of a Stokes regular wave expansion can be written as:

$$\eta(t) = a \cos \varphi(t) + \frac{S_{22}}{d} a^2 \cos 2\varphi(t) + \frac{S_{33}}{d^2} a^3 \cos 3\varphi(t) \quad (4)$$

where  $a$  is the linear wave amplitude,  $d$  is the water depth and  $\varphi(t)$  is the phase. The coefficients  $S_{22}$  and  $S_{33}$  are related to the standard Stokes coefficients defined by Fenton [9] by  $S_{22}/d = kB_{22}$  etc. Stokes expansions are usually written as products of the non-dimensional coefficients with powers of the wavenumber  $k$ , not the undisturbed water depth  $d$ . However, since the intention here is to make use of Stokes theory for irregular wave trains,  $d$  is known (here taken as  $d=70\text{m}$ ), whereas  $k$  would have to be approximated along with  $B_{22}$ . For convenience, the standard Stokes coefficients and the modified versions used here are defined in Appendix A (up to fifth order).

An approximation for the second order sum contribution for an irregular wave will be derived first. For this purpose it is convenient to use a Hilbert transform, which introduces a ninety degrees phase shift into a signal. Thus the Hilbert transform of the linear record  $\eta_L(t)=a(t) \cos\varphi(t)$  is given by:

$$\eta_{LH}(t) = a(t) \sin \varphi(t). \quad (5)$$

where the amplitude,  $a$ , is now assumed to be slowly varying in time. The double frequency contribution can be approximated in terms of the linear record and its Hilbert transform in the form:

$$\eta_2 = a^2 \cos 2\varphi = (\eta_L^2 - \eta_{LH}^2). \quad (6)$$

Similarly, the third order sum contribution is approximated as:

$$\eta_3 = a^3 \cos 3\varphi = \eta_L (\eta_L^2 - 3\eta_{LH}^2). \quad (7)$$

The magnitudes of the second and third order sum contributions are now sought. A number of techniques could potentially be employed to find the coefficients  $S_{22}/d$  and  $S_{33}/d^2$  for use with equations (6) and (7). The approach followed here involves estimating the linear contribution by accounting only for the second order corrections, and then performing a search to find the value of  $S_{22}/d$  that sets the skewness of the linearised time series to zero. From equations (4) and (6) and neglecting the third order contribution (assuming this to be much smaller than the second order contribution), the linear time series can be approximated as:

$$\eta_L(t) \approx \eta(t) - \frac{S_{22}}{d} (\eta_L(t)^2 - \eta_{LH}(t)^2). \quad (8)$$

In order to proceed further it is necessary to make the assumption that the linear record and its Hilbert transform,  $\eta_L$  and  $\eta_{LH}$  in brackets on the right-hand side of equation (8), are approximately equal to the entire measured record and its corresponding Hilbert transform ( $\eta$  and  $\eta_H$ ) respectively. This is a reasonable assumption provided the terms in the Stokes expansion are ordered as  $|\eta_L| \gg |\eta_2| \gg |\eta_3|$ .

Then:

$$\eta_L(t) \approx \eta(t) - \frac{S_{22}}{d} (\eta(t)^2 - \eta_H(t)^2). \quad (9)$$

To obtain  $\eta$  in these expressions the raw data must be high-pass filtered at some suitable cut-off frequency (found through a spectral decomposition of the signal) so as to remove any second order difference (set-down) contribution.

For our purposes here, skewness is most simply defined by the following summation over all data points:

$$\text{Skewness} = \frac{1}{N\sigma^3} \sum_{i=1}^N \eta_L^3 \quad (10)$$

where  $\sigma$  is the standard deviation of the linear record.

The linear record defined by equation (9) can be easily computed and the coefficient  $S_{22}/d$  that results in zero skewness can be found. Because of the variability associated with the New Year wave, together with its highly nonlinear structure, it seems sensible to exclude the New Year wave when computing the coefficient  $S_{22}$  for the 1520 data. For comparison,  $S_{22}$  is computed for the 1520 data both including and excluding the New Year wave. The results yielded from the above analysis for the two Draupner data sets are given in Table 1.

Excluding the New Year wave, the two data sets have a comparable  $S_{22}$  coefficient for zero skewness ( $\sim 1.0$ ). The effect of including the freak wave in the 1520 data increases the size of the second order sum coefficient,  $S_{22}$ , by 41% (from 0.959 to 1.351). Histograms have been plotted for the high-pass filtered 1520 and 1620 data ( $\eta$ ) and the linearised data ( $\eta_L$ ), which has been defined using equation (9) together with the  $S_{22}$  values computed for zero skewness. Figure 5 shows both the histograms of the surface elevation records and their reflections about the origin to help illustrate the degree of skewness present in the data. The plots have been smoothed using a 29-point average to help reveal the underlying shapes. For the 1620 record all data points were considered, whereas for the 1520 record data points within a 45 second interval centred at the New Year wave were excluded. Upon linearising the data the histograms and their reflections are found to overlie almost exactly. If all of the 1520 data points are considered and a  $S_{22}$  value of 1.351 is used, the resulting histogram and its reflection for the linearised data still show considerable mismatch. In the context of a short record of  $\sim 100$  waves, the New Wave is indeed extraordinary!

For comparison with Figure 3, Figure 6 shows a plot of ordered crest elevation against ordered trough depression for the linearised Draupner wave records, again computed using equation (9) and the  $S_{22}$  values found for zero skewness. With the exception of the largest values in each ordered data set, the plots now show comparatively little asymmetry, deviating only slightly from the 1:1 line for all crest and trough sizes.

The reasoning behind the re-definition of the Stokes expansion coefficients is now explained. When approximating the nonlinear components in a measured wave record, the choice of the wavenumber  $k$  is ambiguous. Some possibilities are: (1) Use a wavenumber value based on the peak frequency (i.e. the frequency of the most energetic waves); (2) Use a wavenumber value based on the mean zero-crossing frequency; (3) Use a local time-varying wavenumber value based on an instantaneous effective frequency at each point in the record. Here an alternative approach is used whereby a single  $kd$  (wavenumber-depth product) value is sought through a comparison of the  $S_{22}/d$  value computed for zero skewness with the appropriate Stokes second order coefficient,  $S_{22}/d$  (as defined in Appendix A). The computed value of  $kd$  can then be used to estimate the third order Stokes coefficient,  $S_{33}/d^2$  (and higher order coefficients if required).

Upon estimating the  $S_{22}/d$  coefficients for zero skewness, it was found that a suitable  $kd$  value for use in the computation of the third order Stokes coefficient is 1.6. To help illustrate the reasoning for this decision, Figure 7 plots the variation of the theoretical Stokes coefficients,  $S_{22}$  and  $S_{33}$ , with  $kd$ , and also shows two horizontal lines corresponding to the values of  $S_{22}$  found for zero skewness (the horizontal line drawn for the 1520 data is for the case where the New Year wave has been excluded). From

this figure it is clear that, for this particular water depth (70m), both the second and third order coefficients,  $S_{22}$  and  $S_{33}$ , are relatively insensitive to the exact  $kd$  value used in the calculation. A  $kd$  value of 1.6 corresponds to the minimum of the  $S_{22}$  curve and a wave period of 13.8 seconds; which is sufficiently close to the average wave period,  $T_z$ , of 12.5 seconds for such a wavenumber to be deemed reasonable. The choice of a suitable wavenumber will be considered further later when discussing exact second order wave theory.

Using a  $kd$  value of 1.6, the second and third order sum coefficients,  $S_{22}$  and  $S_{33}$ , are found to be 1.10 and 1.57 respectively (using equations A3 and A5, Appendix A). Hence the first three terms in the Stokes wave expansion for the Draupner data can be approximated as:

$$\eta(t) = a \cos \varphi + \frac{1.10}{70} a^2 \cos 2\varphi + \frac{1.57}{70^2} a^3 \cos 3\varphi. \quad (11)$$

The slight discrepancy between the values of  $S_{22}$  found for zero skewness ( $S_{22} \sim 1.0$ ) and the value computed using  $kd=1.6$  ( $S_{22}=1.10$ ) can be attributed to the relatively small effect of directional spreading on the magnitude of second order sum contributions (Forristall [10]).

## 5. Fifth order NewWave

When the linear NewWave profile is compared against the New Year wave profile, considerable mismatch is found. The NewWave model is now modified to include nonlinear corrections up to fifth order using the theory outlined in Appendix A;

modified versions of the Stokes coefficients defined by Fenton [9] are used and suitable expressions for the temporal contributions for all nonlinear terms up to fifth order have been derived using the linear wave record and its Hilbert transform. For the estimation of the Stokes coefficients  $kd=1.6$  has again been used. Figure 8 plots the fifth order NewWave profile together with its first, second and third order contributions (fourth and fifth order contributions have been excluded as they are too small to clearly illustrate graphically). Figure 8 also shows a comparison between the fifth order NewWave and the New Year wave. A linear NewWave amplitude of 14.7m is used as this corresponds to an amplitude of 18.5m in the fifth order corrected NewWave profile, matching the amplitude of the measured New Year wave. This comparison does not incorporate any representation of the second order difference contribution. This is discussed in Sections 7, 8 and 9.

The effects of including nonlinear contributions are largely as one would expect; the crests become narrowed and raised, while the troughs are broadened and raised. As one would expect, the size of the nonlinear contributions decreases rapidly as the order increases. Beyond second order, the effects of non-linearity are most pronounced close to the apex of a crest; the crest is sharpened further. Quantitatively, by including nonlinear corrections up to fifth order, the peak crest of the NewWave profile has been raised by 26% (from 14.7m to 18.5m) whereas the deepest troughs have been raised by 17% (from 10.0m to 8.3m). The agreement between the fifth order NewWave profile and the New Year wave profile close to the peak is surprisingly good, with the broad banded nature of the freak wave being captured quite well. The troughs either side of the peak crest are still predicted to be too deep;

the actual trough depths are 6.5m and 7.1m. Hence the New Year wave is slightly broader banded, having shallower troughs and lower crests adjacent to the main peak.

Assuming the standard Rayleigh distribution for linear crest amplitude and taking the linear crest amplitude to be 14.7m, it is found that the New Year wave is approximately a 1 in  $2 \times 10^5$  wave for this particular sea state (with a significant wave height of ~12m).

## **6. Spectral decomposition**

Spectral analysis will now be used to assist in decomposing a wave record into its constituent components. The Draupner 1520 data set will be considered here.

It is obviously difficult to identify the frequency range over which the linear and higher order contributions are significant. Hence it is useful to decompose the data in the time domain into its constituent components and then Fourier transform each component individually to obtain estimates for the isolated spectral contributions. Spectra for the estimated second order difference, second order sum and third order sum contributions are examined.

Approximations for the temporal contributions to the second and third order sum terms are defined in equations (6), (7). An approximation for the second order difference contribution can be obtained using the ideas of multiple-scales analysis (Bender and Orszag [11]) to specifically define  $a(t)$  to be a slowly varying function of time with a time scale comparable to the second order difference contribution, and

$\varphi(t)$  to be a fast phase variation. As for the second and third order sum contributions, the slowly varying envelope function  $a(t)$  can be expressed in terms of the linear record and its Hilbert transform as:

$$a(t) = \sqrt{\eta_L(t)^2 + \eta_{LH}(t)^2} . \quad (12)$$

The spectrum of the wave envelope defined by equation (12) can be used to estimate the frequency range of the second order difference contribution.

The overall wave spectrum and estimated spectra for the second order difference, second order sum and third order sum contributions are shown in Figure 9. In order to remove some of the statistical variability in the data, smoothed spectra have been produced using a 15-point running average. This averaging process causes a slight broadening of the spectra. The aim here is to separate the various contributions in the frequency domain and to find the range of frequencies over which each contribution is present. Therefore, true power values are not of interest and so the vertical scale for each spectrum has been normalised such that the maximum peak of each is unity.

As is shown in Figure 9, the approach outlined clearly identifies the range of frequencies over which each contribution is present and hence has been a success. In addition, the spectral decomposition undertaken helps to partly justify the narrow-banded Stokes-type treatment adopted in this study since the second order difference, second order sum and third order sum contributions are reasonably well separated in frequency.

## 7. Second order difference contribution

The second order difference contribution will now be investigated for the largest waves in the two Draupner wave records. From a spectral decomposition of the data (as shown above for the 1520 data), it is found that the second order difference contribution can be extracted by low-pass filtering the data at 0.04Hz (for both the 1520 and 1620 data) - i.e. set all frequency components above this cut-off value to zero. This cut-off frequency has been chosen so as to maximise the second order difference contribution and minimise the linear contribution that is passed through the filter. Time series plots for the largest waves in the Draupner 1520 and 1620 data sets together with their presumed second order difference contributions for three different filtering frequencies are shown in Figure 10.

For the largest wave in the 1620 data, the second order difference contribution is found to have a negative value (i.e. there is a set-down in the second order difference contribution). This set-down remains for progressively lower filtering frequencies. This is what one would expect for a large free wave on the open sea and is observed for all large waves (largest 10%) analysed in the two Draupner data sets, with the exception of the New Year wave. The second order difference contribution to the New Year wave exhibits a substantial set-up (i.e. has a positive value), which is entirely unexpected. One might conclude that some linear contribution must have passed through the filter causing the apparent set-up. However, this hypothesis is soon dispelled through low-pass filtering at progressively lower frequencies, where one still finds the set-up present. No explanation of this anomalous behaviour can be offered at this time.

It is worth noting that the peak second order difference contribution to a wave will not necessarily coincide exactly with the occurrence of the wave peak, and this is illustrated in Figure 10 for the largest wave in the 1620 data. The reason for this is that the peak second order difference contribution will occur at the instance of the maximum in the envelope signal,  $a(t)$ , rather than the maximum of the higher frequency signals constrained by the envelope.

## 8. Second order difference model

As a first approximation to the second order difference contribution the following equation can be used (Dean and Dalrymple [12]):

$$\eta_{2-} = -\frac{a^2 k}{2 \sinh 2kd} \quad (13)$$

where  $d$  is the water depth. This equation represents the wave self-interaction component of the total second order difference contribution (see Dalzell [6]). The envelope function in this approximation can be defined using equation (12) so long as the mean square value of this function is removed. Hence an approximation for the second order difference contribution is given by:

$$\eta_{2-} = -\frac{k}{2 \sinh 2kd} \left( a^2 - \overline{a^2} \right). \quad (14)$$

Figure 11 compares the low-pass filtered second order difference contribution (using a cut-off frequency of 0.04Hz) to the Draupner 1520 data with the approximation defined by equation (14). In Figure 11, the vertical scale of the approximation is arbitrarily set to allow the set-down predicted for the New Year wave to have the same magnitude as the actual set-up found in the data. This very crude long wave approximation has managed to capture the position of most of the long bound wave set-ups and set-downs in the filtered profile. Note the alignment of the deepest set-down at ~1170 seconds, corresponding to the time of occurrence of the second largest wave in the 1520 record. However, close to the New Year wave at ~265 seconds there is a complete mismatch. As is clear from the figure, no suitable scaling factor can be found to allow all the peak values to be reproduced exactly.

## **9. Exact second order wave theory**

Exact second order wave theory, as outlined by Dean and Sharma [5] and more recently by Dalzell [6], is now used to help assess the magnitude and character of the second order difference contribution further. In addition, to help validate the approximation procedure for nonlinear contributions implemented in this study, comparisons will be drawn between the second order sum contribution computed using exact second order wave theory and that approximated in terms of the linear record and its Hilbert transform (equation (6)).

From measured spectra, second order contributions based on NewWave profiles for both the Draupner 1520 and 1620 data sets have been computed. The second order equations given by Dalzell [6] are defined for two linear wave components. The

simulation of a NewWave surface profile defined by  $N$  linear components involves the summation of  $N$  second order Stokes waves together with the summation of the  $O(N^2)$  wave-wave interaction components for all possible pairs of different linear wave components.

As before, the largest waves in the Draupner 1520 and 1620 data sets are considered here. The linear amplitude of each wave is taken to be the linear NewWave amplitude required to produce a fifth order NewWave amplitude equal to the total wave amplitude (as is illustrated in Figure 8 for the New Year wave). Assuming unidirectional wave motion, Figure 12 shows the second order sum and difference contributions to each wave calculated using exact second order wave theory. These second order contributions will be compared against an approximation for the second order sum contribution (equation (6) together with the coefficient  $S_{22}/d$ , computed using  $k=1.6/d$ ) and the low-pass filtered second order difference contribution (obtained using a cut-off frequency of 0.04Hz). Table 2 summarises these comparisons.

For both data sets the second order sum approximation,  $\eta_{2A+}$ , agrees very well with the value computed using full second order wave theory,  $\eta_{2T+}$ ; to one decimal place the values agree exactly. From Table 2, the second order sum coefficients,  $S_{22}$ , computed using exact second order wave theory are found to be 0.90 and 0.87 for the Draupner 1520 and 1620 data sets respectively. These values are close to those computed earlier for zero skewness ( $S_{22}\sim 1$ ). This comparison helps to validate the approximation procedure adopted in this study, namely to express all nonlinear contributions in terms of the linear wave record and its Hilbert transform. The

agreement here also confirms that it was reasonable to define  $kd=1.6$  for the calculation of the Stokes coefficients presented in this paper.

The second order difference contribution to the largest wave in the 1620 data defined by exact second order wave theory,  $\eta_{2T}$ , is relatively close to the low-pass filtered value,  $\eta_{2F}$ , observed in the data. The discrepancy can be attributed to directional spreading of the linear wave components, which is known to reduce the magnitude of the second order difference set-down beneath an energetic group (Forristall [10]). In stark contrast, for the New Year wave, a set-down of -1.12m is predicted by second order wave theory although the data exhibits a set-up in the apparent second order difference contribution of +0.48m. An observed set-up in wave measurements around a large structure could be attributed to nonlinear wave diffraction, but since the Draupner platform is a steel space-frame structure this explanation is unlikely to be valid here. Whilst a broadening of the spectral peak during a sufficiently steep focus event is well known to occur due to third order Benjamin-Feir wave-wave interactions (Yuen and Lake [13], Peregrine [14], Baldock, Swan and Taylor [15]), filtering of the low frequency wave components in the measured wave record with progressively lower cut-off frequencies (0.04, 0.03, 0.02Hz) shows that this set-up is a robust feature remaining at very low frequencies. To the authors' knowledge, this study is the first to identify such anomalous behaviour in this extraordinary wave.

## **10. Conclusions**

Field data from the North Sea has been used to explore the shapes of large surface waves. NewWave has been proposed as a reasonable model for the linear contribution

to large waves. Stokes-type corrections have been used to approximate the non-linear bound harmonics present, and a technique has been developed that enables the magnitude of the second and higher order contributions to a wave record to be estimated.

Unique features of the Draupner New Year wave have been identified distinguishing it from a typical large wave. A fifth order NewWave profile reproduces the New Year wave reasonably well close to the peak, although is still too narrow banded. By linearising the New Year wave profile, its probability of occurrence is estimated to be 1 in  $2 \times 10^5$  waves – an unlikely but obviously not impossible event in a record containing ~100 waves!

As one would expect for a large wave in the open sea, exact second order wave theory predicts a large set-down in the second order difference contribution to the New Year wave. The field data exhibits an anomalous set-up for the New Year wave, whereas all the other large waves show a local set-down. Unexplained behaviour such as this prompts the suggestion that new physics, not incorporated in standard approaches to offshore engineering design, is likely to have played an important role in the generation of this freak wave.

## **11. Acknowledgements**

The authors would like to thank Dr. Sverre Haver of Statoil for kindly providing the data studied here. The first author is supported through an EPSRC-Shell industrial CASE award.

## Appendix A: Stokes fifth order wave theory

Stokes assumed that the properties of a regular wave can be represented by Fourier series and that the coefficients in these series can be written as perturbation expansions in terms of a parameter that increases with wave height. Substitution of the perturbation expansions into the governing equations defining the water wave problem and manipulation of the series yields the solution. Stokes wave theory is presented to fifth order here using the results derived by Fenton [9].

The fifth order free surface elevation,  $\eta(x,t)$ , measured from the mean water level, is given by:

$$k\eta = \sum_{i=1}^5 \varepsilon^i \sum_{j=1}^i B_{ij} \cos jk(x-ct) + \dots \quad (\text{A1})$$

where  $\varepsilon=ka$ ,  $k$  is the wavenumber and  $a$  is the wave amplitude. The coefficients  $B_{ij}$  can be expressed in terms of hyperbolic functions of  $kd$ , where  $d$  is the water depth, as:

$$B_{11} = 1 \quad (\text{A2})$$

$$B_{22} = \frac{\coth kd(1+2C)}{2(1-C)} \quad (\text{A3})$$

$$B_{31} = \frac{3(1+3C+3C^2+2C^3)}{8(1-C)^3} \quad (\text{A4})$$

$$B_{33} = -B_{31} \quad (\text{A5})$$

$$B_{42} = \frac{\coth kd(6 - 26C - 182C^2 - 204C^3 - 25C^4 + 26C^5)}{6(3 + 2C)(1 - C)^4} \quad (\text{A6})$$

$$B_{44} = \frac{\coth kd(24 + 92C + 122C^2 + 66C^3 + 67C^4 + 34C^5)}{24(3 + 2C)(1 - C)^4} \quad (\text{A7})$$

$$B_{51} = -(B_{53} + B_{55}) \quad (\text{A8})$$

$$B_{53} = \frac{9(132 + 17C - 2216C^2 - 5897C^3 - 6292C^4 - 2687C^5 + 194C^6 + 467C^7 + 82C^8)}{128(3 + 2C)(4 + C)(1 - C)^6} \quad (\text{A9})$$

$$B_{55} = \frac{5(300 + 1579C + 3176C^2 + 2949C^3 + 1188C^4 + 675C^5 + 1326C^6 + 827C^7 + 130C^8)}{384(3 + 2C)(4 + C)(1 - C)^6} \quad (\text{A10})$$

where  $C = \text{sech}^2 kd$ .

Now, dividing through by  $k$  and introducing the modified Stokes coefficients,  $S_{ij}$ , equation A1 can be expressed in the form:

$$\begin{aligned} \eta = & S_{11}D_{11} + \frac{S_{22}}{d}D_{22} + \frac{S_{31}}{d^2}D_{31} + \frac{S_{33}}{d^2}D_{33} + \frac{S_{42}}{d^3}D_{42} + \frac{S_{44}}{d^3}D_{44} + \frac{S_{51}}{d^4}D_{51} \\ & + \frac{S_{53}}{d^4}D_{53} + \frac{S_{55}}{d^4}D_{55} \end{aligned} \quad (\text{A11})$$

where the newly introduced  $D$  variables contain both the amplitude and phase information and are defined in terms of the linear wave record and its Hilbert transform,  $\eta_L$  and  $\eta_{LH}$  respectively:

$$D_{11} = a \cos \theta = \eta_L \quad (\text{A12})$$

$$D_{22} = a^2 \cos 2\theta = \eta_L^2 - \eta_{LH}^2 \quad (\text{A13})$$

$$D_{31} = a^3 \cos \theta = (\eta_L^2 + \eta_{LH}^2) \eta_L \quad (\text{A14})$$

$$D_{33} = a^3 \cos 3\theta = (\eta_L^2 - 3\eta_{LH}^2) \eta_L \quad (\text{A14})$$

$$D_{42} = a^4 \cos 2\theta = (\eta_L^2 + \eta_{LH}^2)(\eta_L^2 - \eta_{LH}^2) \quad (\text{A15})$$

$$D_{44} = a^4 \cos 4\theta = (\eta_L^2 - \eta_{LH}^2)^2 - (2\eta_L \eta_{LH})^2 \quad (\text{A16})$$

$$D_{51} = a^5 \cos \theta = (\eta_L^2 + \eta_{LH}^2)^2 \eta_L \quad (\text{A17})$$

$$D_{53} = a^5 \cos 3\theta = (\eta_L^2 + \eta_{LH}^2)(\eta_L(\eta_L^2 - 3\eta_{LH}^2)) \quad (\text{A18})$$

$$D_{55} = a^5 \cos 5\theta = ((\eta_L^2 - \eta_{LH}^2)^2 - (2\eta_L \eta_{LH})^2) \eta_L - 4\eta_{LH}^2 \eta_L (\eta_L^2 - \eta_{LH}^2). \quad (\text{A19})$$

## References

1. Lindgren, G, 1970, Some properties of a normal process near a local maximum, *Ann. Math. Statist.* 41, pp.1870-1883.
2. Boccotti, P, 1983, Some new results on statistical properties of wind waves, *Applied Ocean Research* 5, pp.134-140.
3. Haver, S., and Jan Andersen, O., 2000, Freak waves: rare realizations of a typical population or typical realizations of a rare population?, *Proceedings of the tenth International Offshore and Polar Engineering conference*, Seattle USA.
4. Prevosto, M., and Bouffandeau, B., 2002, Probability of occurrence of a “giant” wave crest, *Proceedings of OMAE2002* 28446.
5. Dean, R.G., and Sharma, J.N., 1981, Simulation of wave systems due to nonlinear directional spectra, *Int. Symp. on Hydrodynamics in Coastal Engineering*, Trondheim, Norway, pp.1211-1222.
6. Dalzell, J.F., 1999, A note on finite depth second-order wave-wave interactions, *Applied Ocean Research* 21, pp105-111.

7. Jonathan, P., and Taylor, P.H., 1997, On irregular, non-linear waves in a spread sea, *J. Offshore Mechanics and Arctic Engineering* 119, pp.37-41.
8. Taylor, P.H., and Williams, B.A., 2004, Wave statistics for intermediate water depth – NewWaves and symmetry, *Trans. of the ASME*, Vol. 126, pp.54-59.
9. Fenton, J., *Nonlinear Wave Theories*, 1990, *The Sea, Volume 9 - Ocean Engineering Science*, John Wiley and Sons Ltd, pp 3-25.
10. Forristall, G.Z., 1999, Wave crest distributions: Observations and second-order theory, *J. Physical Oceanography* 30, pp.1931-1943.
11. Bender, C.M., and Orszag, S.A., 1978, *Advanced mathematical methods for scientists and engineers*, McGraw-Hill.
12. Dean, R.G., and Dalrymple, R.A., 1991, *Water wave mechanics for engineers and scientists*, World Scientific.
13. Yuen, H.C., and Lake, B.M., 1982, Nonlinear dynamics of deep water gravity waves, *Advances in applied mechanics* (ed. Chia-Shun Yih) 22, London, pp.153-180.
14. Peregrine, D.H., 1983, Water waves, nonlinear Schrodinger equations and their solutions, *J. Austral. Math. Soc. B*25, pp.16-43.
15. Baldock, T.E., Swan, C., and Taylor, P.H., 1996, A laboratory study of nonlinear surface waves on water, *Phil. Trans. Roy. Soc. A*354, pp.649-676.

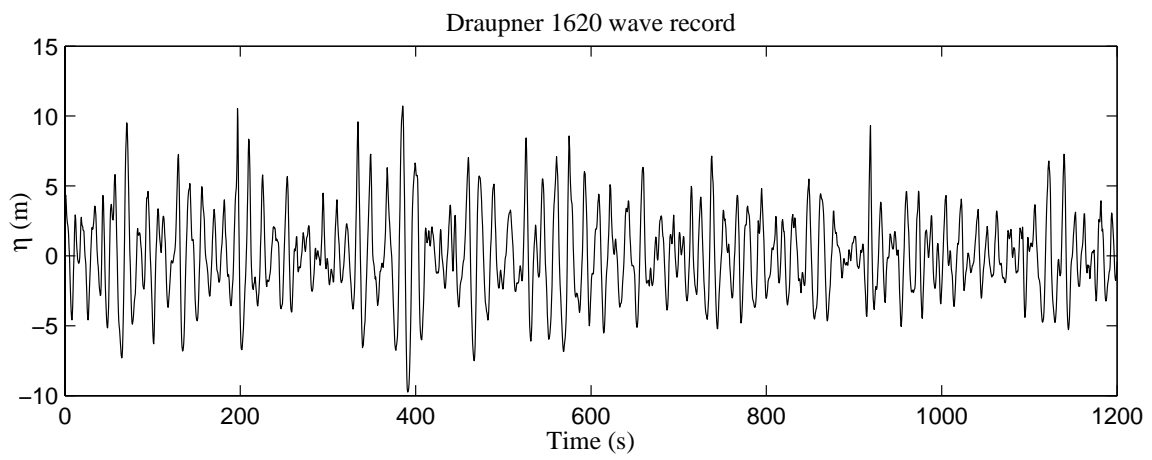
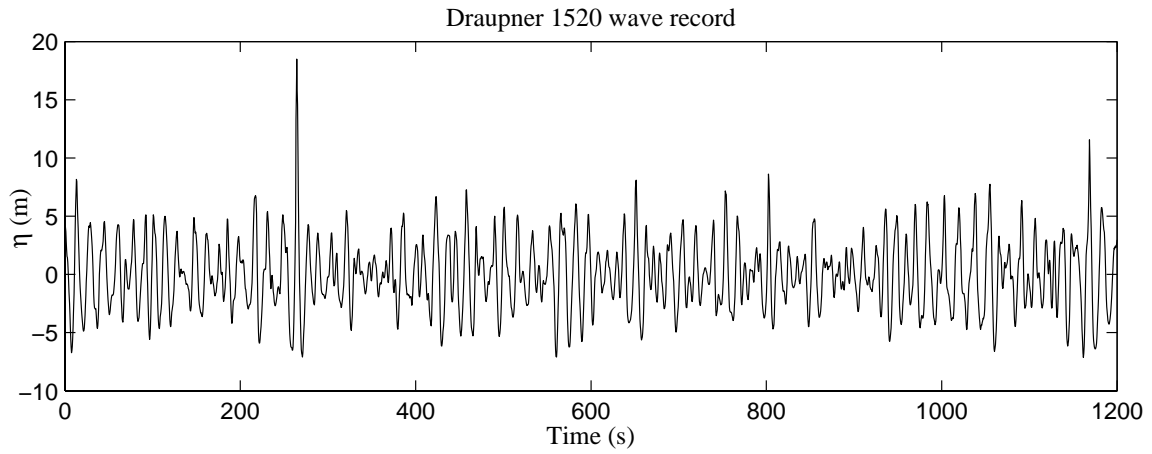


Figure 1. Time series plots for the Draupner 1520 and 1620 wave records.

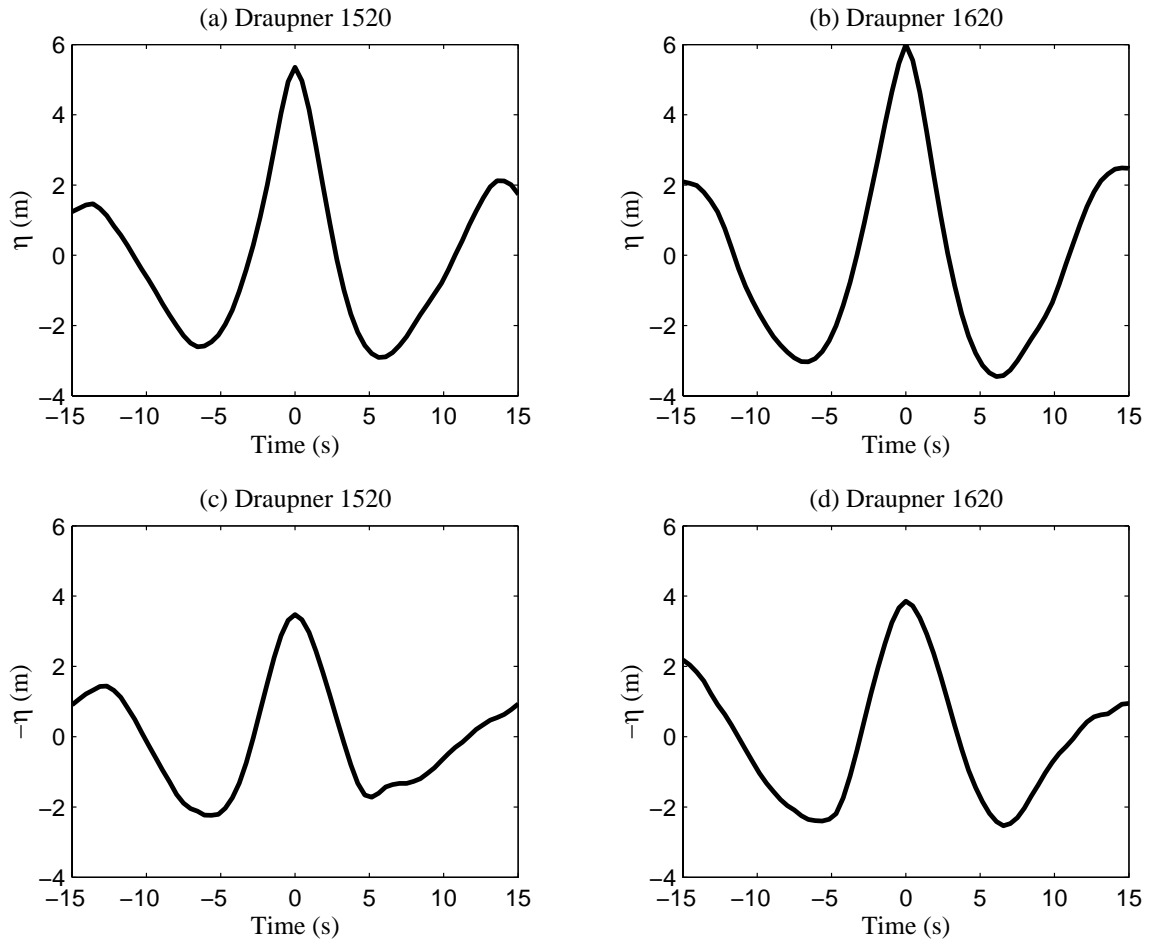


Figure 2. Average large crest, (a)-(b), and average large trough, (c)-(d), profiles for the Draupner 1520 and 1620 wave records.

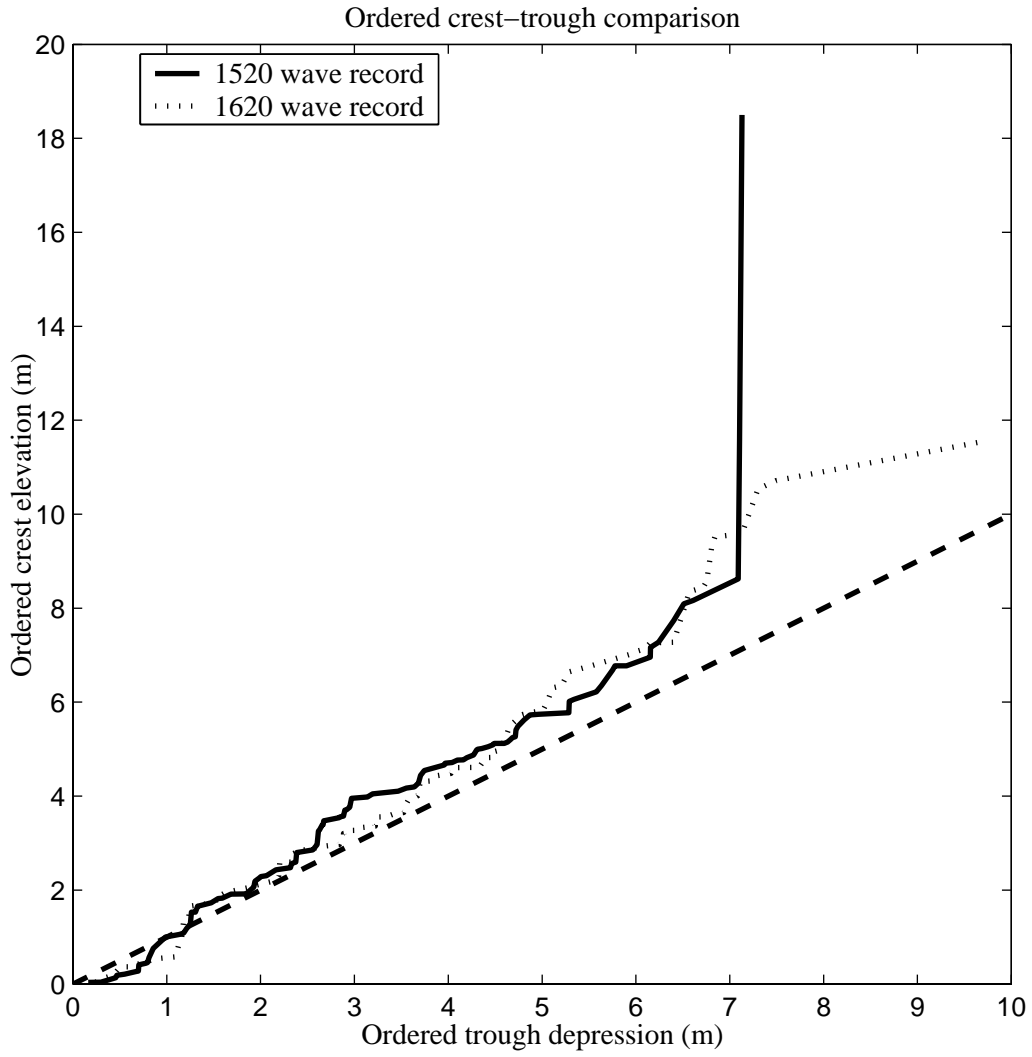


Figure 3. Ordered crest elevation plotted against ordered trough depression for the Draupner 1520 and 1620 wave records. A 1:1 line is shown (dashed line).

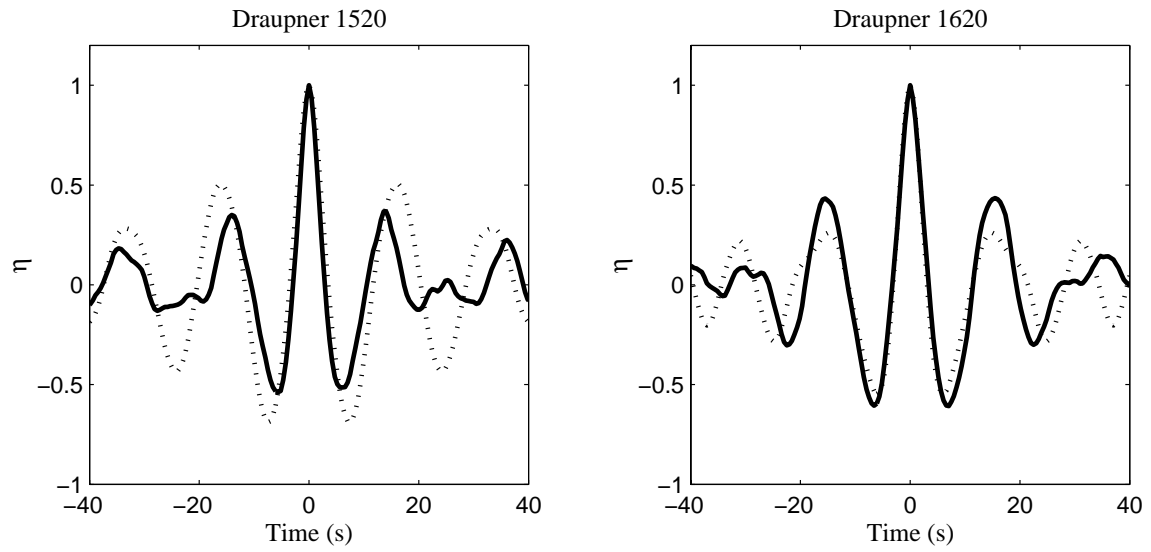


Figure 4. Comparison of the average linear large crest profile with the linear NewWave profile for the two Draupner wave records. Solid line: average linear profile. Dotted line: linear NewWave profile. The crest amplitudes have been normalised such that the peak crest elevations equal 1.

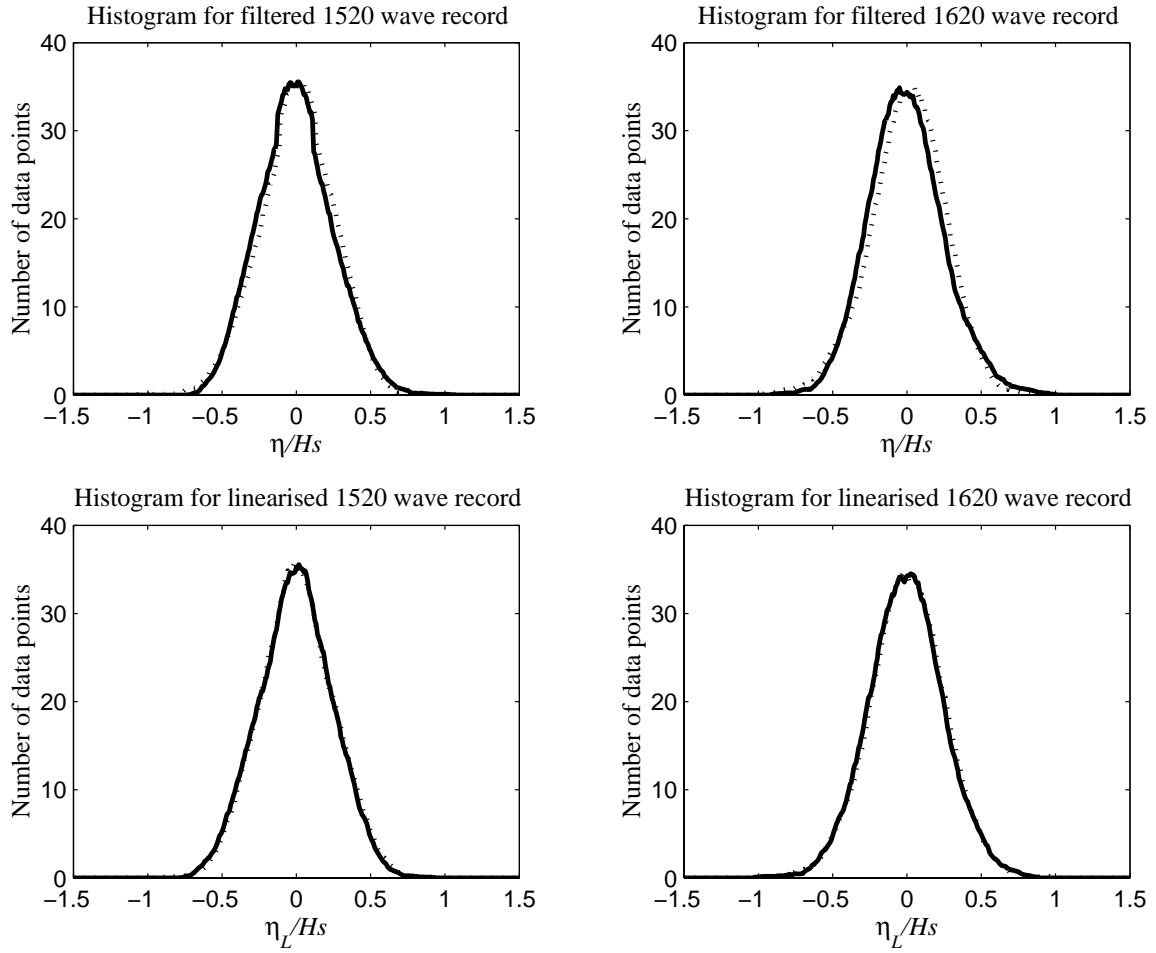


Figure 5. Histograms (solid lines) with their reflections about the origin superimposed on top (dotted lines) for the high-pass filtered data ( $\eta$ ) and the linearised data ( $\eta_L$ ). Surface elevation has been normalised by dividing through by the significant wave height,  $H_s$ . All data points have been considered except those within a 45 second interval around the New Year wave in the 1520 data.

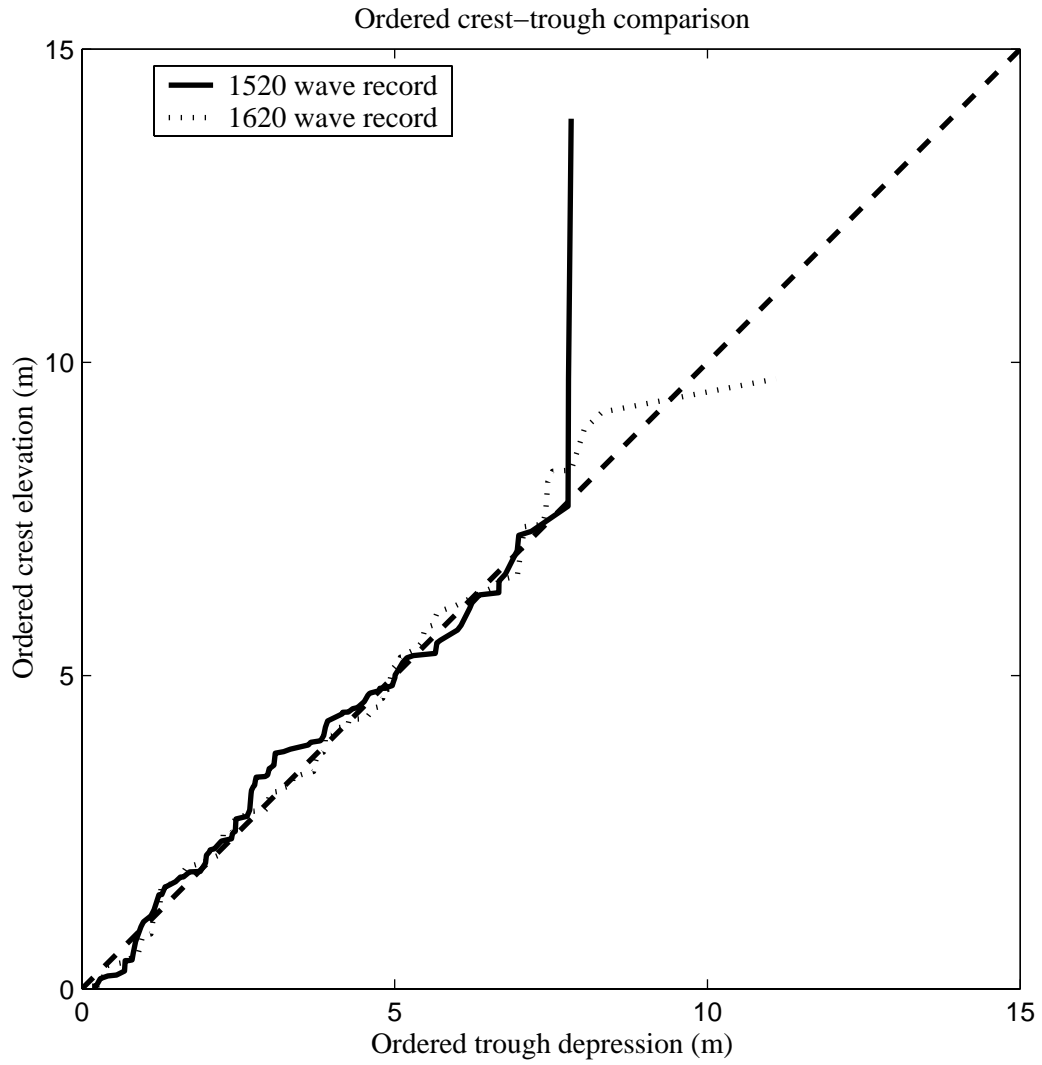


Figure 6. Ordered crest elevation plotted against ordered trough depression for the linearised Draupner 1520 and 1620 wave records. A 1:1 line is shown (dashed line).

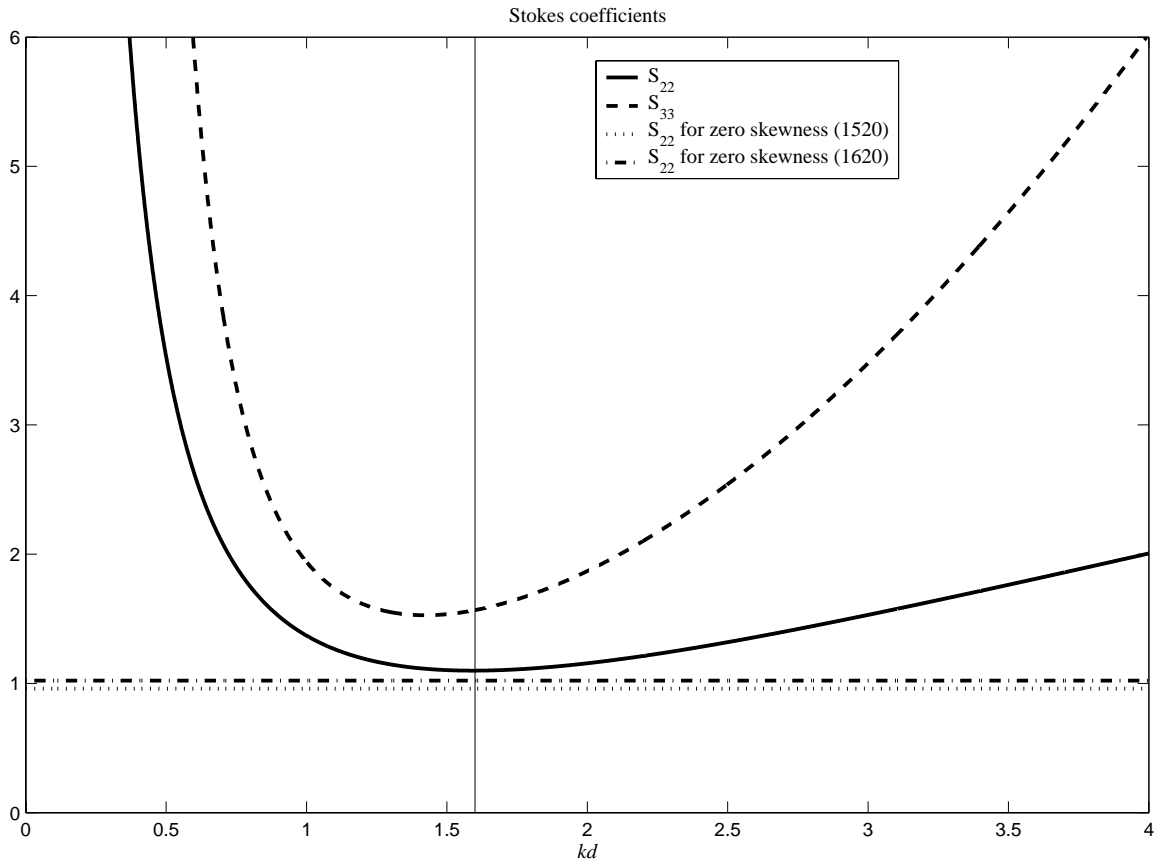


Figure 7. Stokes second and third order sum coefficients,  $S_{22}$  and  $S_{33}$ , plotted against  $kd$ . Horizontal lines are shown corresponding to the  $S_{22}$  values computed for zero skewness. A vertical line is drawn at  $kd=1.6$ .

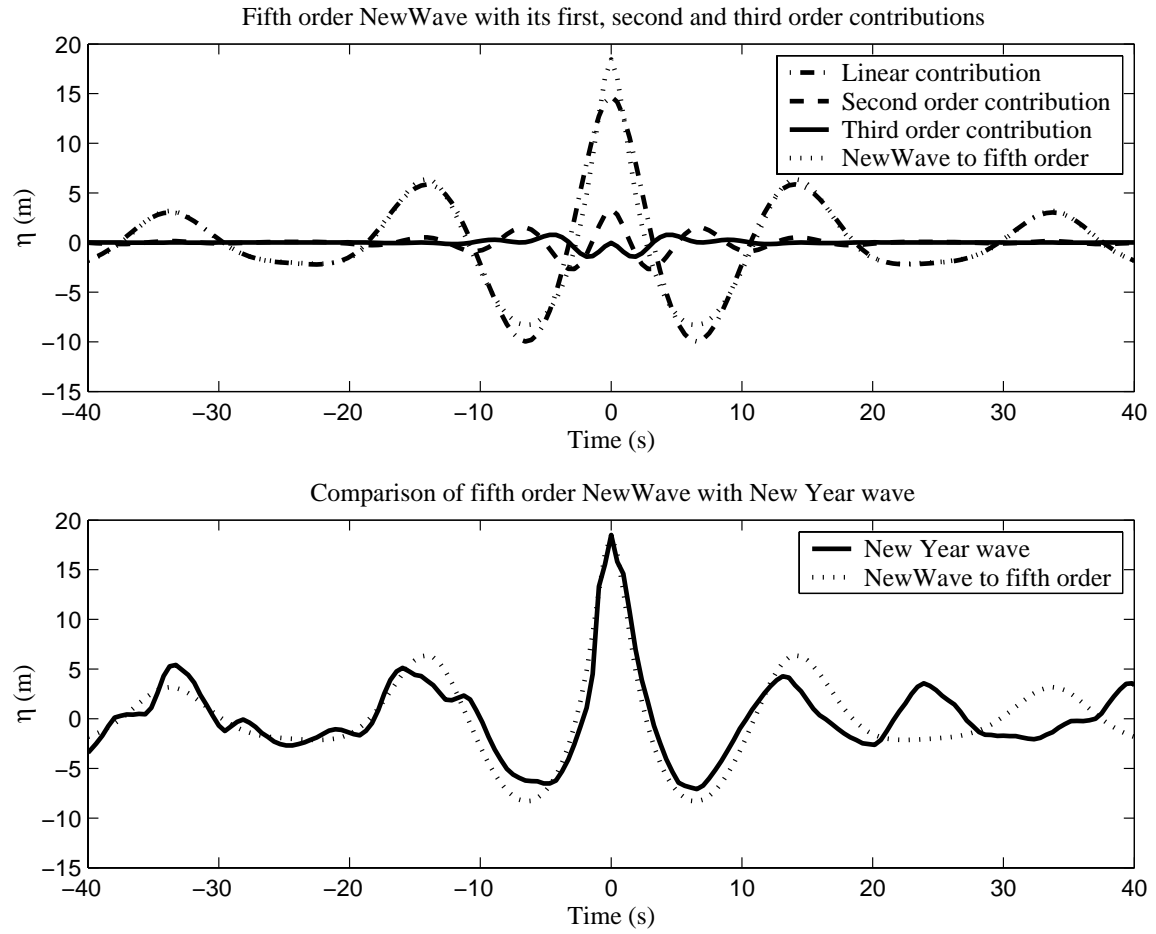


Figure 8. A comparison of the fifth order NewWave profile with its constituent contributions (first, second and third order only) and the New Year wave.

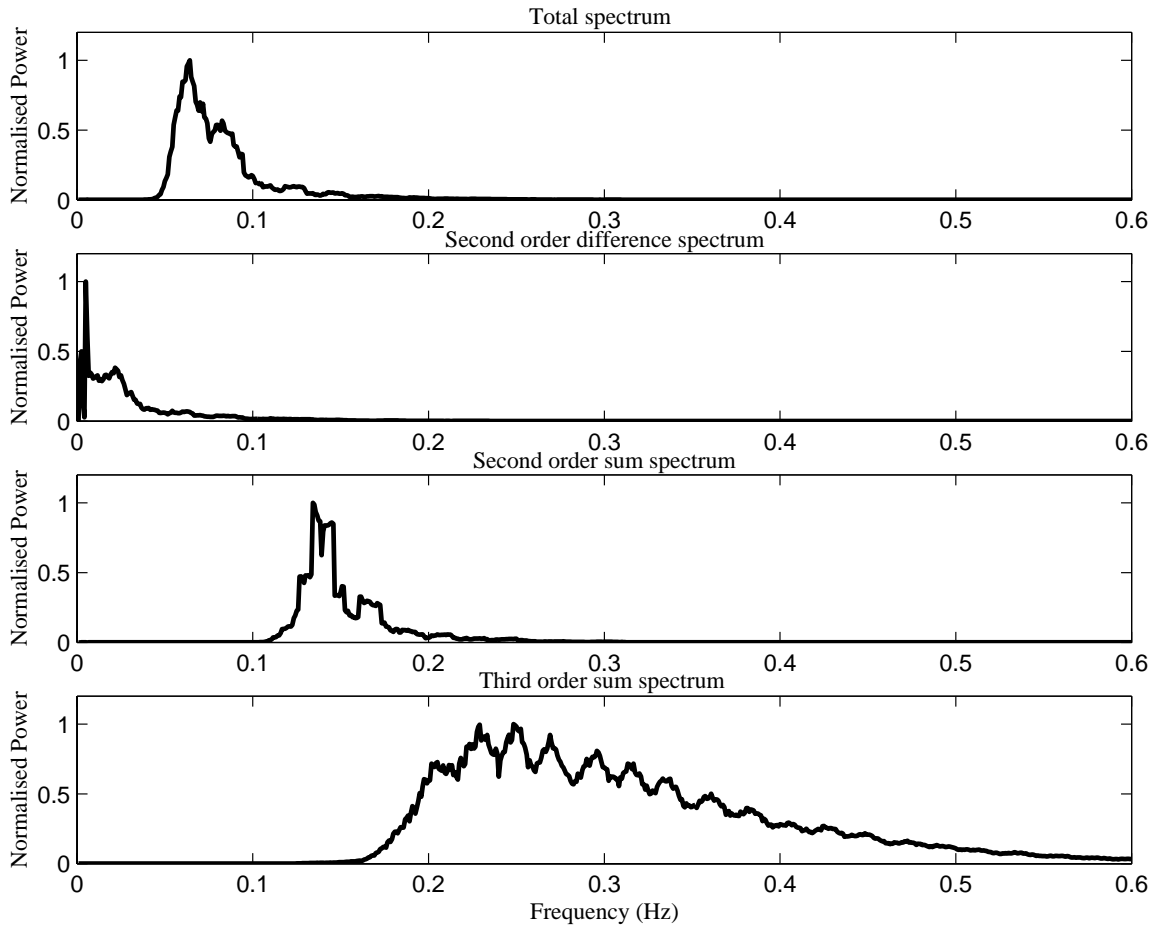


Figure 9. Smoothed power spectra for the Draupner 1520 wave record.

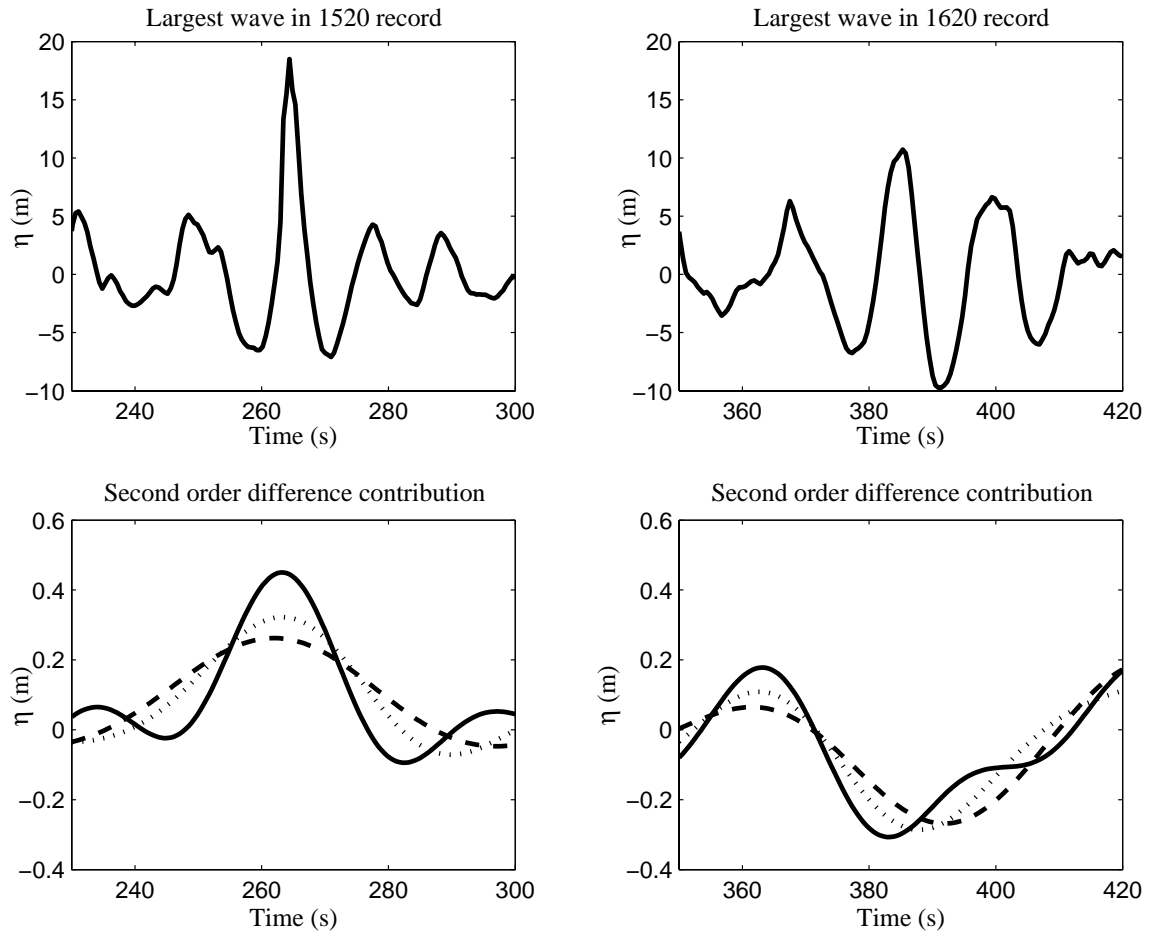


Figure 10. Time series plots for the largest waves in the Draupner 1520 and 1620 wave records together with their second order difference contributions (positioned beneath) for three different filtering frequencies; 0.04Hz (solid line), 0.03Hz (dotted line) and 0.02Hz (dashed line).

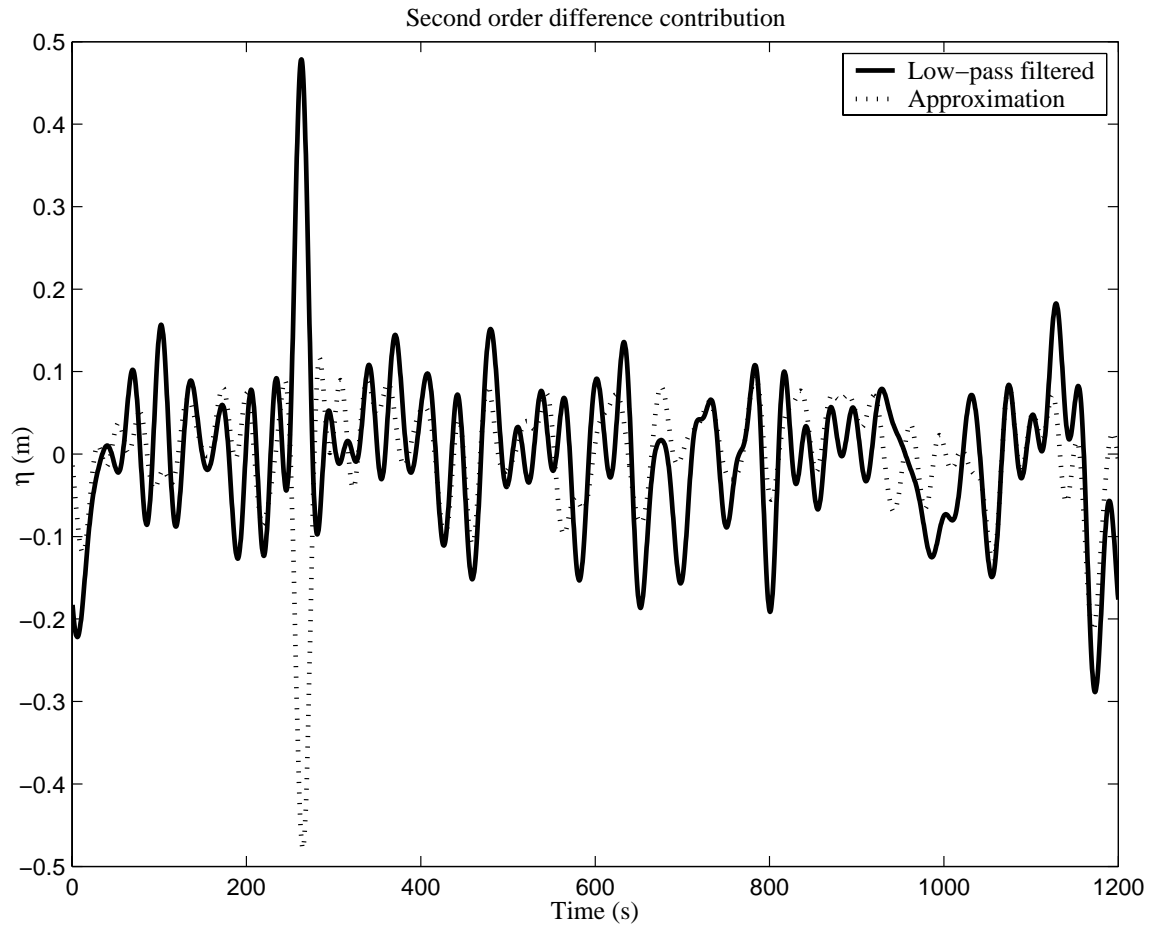


Figure 11. Approximation for the second order difference contribution to the Draupner 1520 wave record.

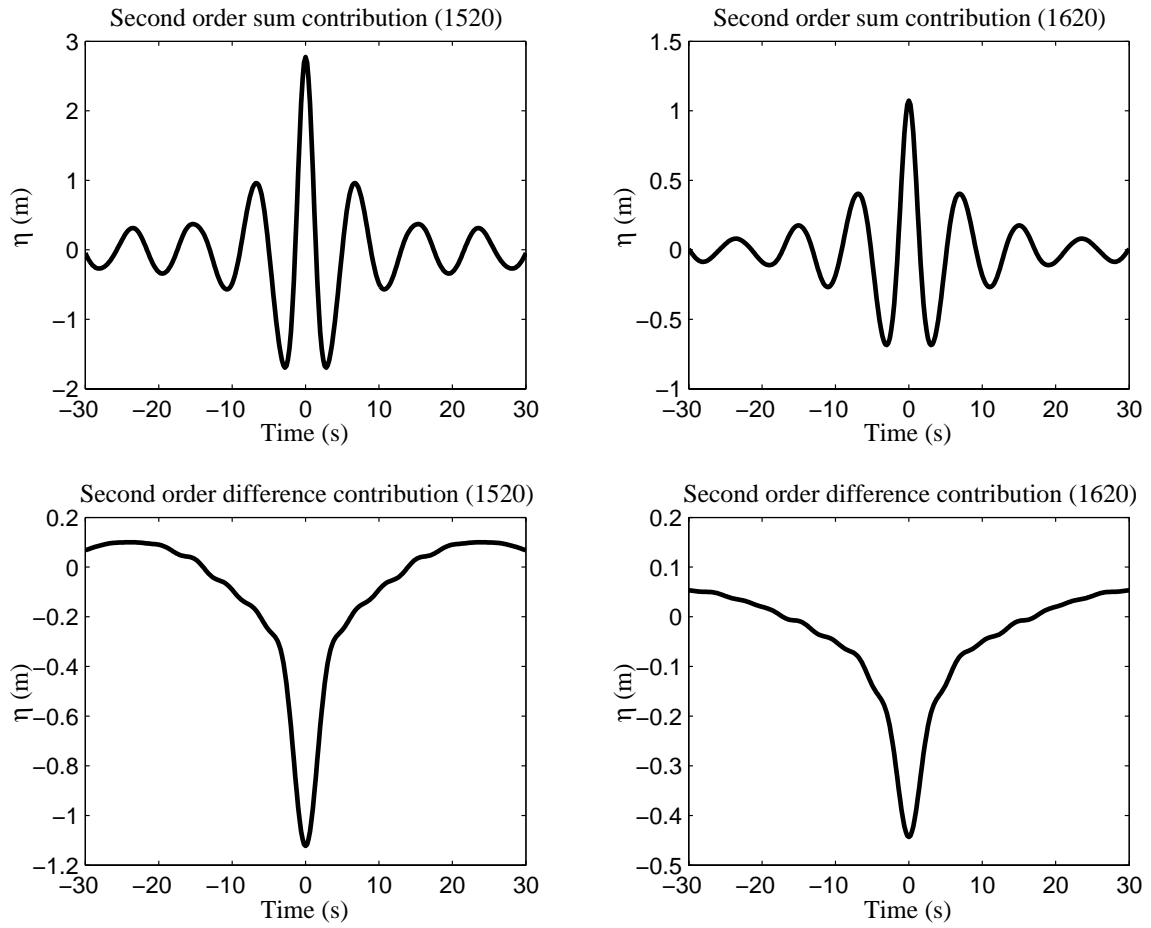


Figure 12. Second order sum and difference contributions for the largest waves in the Draupner 1520 and 1620 wave records calculated using exact second order wave theory.

Data set	$S_{22}$ for zero skewness
Draupner 1620	1.022
Draupner 1520 (including freak wave)	1.351
Draupner 1520 (excluding freak wave)	0.959

Table 1. Table of second order coefficient values for the Draupner 1520 and 1620 wave records.  $S_{22}$  values are given to three decimal places.

Wave	$\eta_{2A+}$	$\eta_{2T+}$	$\eta_{2F-}$	$\eta_{2T-}$
Largest wave in 1520 record	+2.82	+2.77	+0.48	-1.12
Largest wave in 1620 record	+1.13	+1.07	-0.34	-0.44

Table 2. Table comparing second order contributions for the largest waves in the Draupner 1520 and 1620 wave records.  $\eta_{2A+}$  is the second order sum approximation.  $\eta_{2F-}$  is the filtered second order difference contribution.  $\eta_{2T+}$  and  $\eta_{2T-}$  are the second order sum and difference contributions respectively calculated using exact second order wave theory. Values given are in metres (m).